Brain Stimulation 13 (2020) 35–46

Contents lists available at ScienceDirect

Brain Stimulation

journal homepage: http://www.journals.elsevier.com/brain-stimulation

Transcranial focused ultrasound pulsation suppresses pentylenetetrazol induced epilepsy *in vivo*

Sin-Guang Chen [a, b, 1], Chih-Hung Tsai [a, 1], Chia-Jung Lin [a], Lee Cheng-Chia[c, d], Hsiang-Yu Yu [d, h], Tsung-Hsun Hsieh [e, f, i, **], Hao-Li Liu [a, g, *]

[a] Department of Electrical Engineering, Graduate Institute of Clinical Medical Sciences, Chang Gung University, Taoyuan, Taiwan
[b] Department of Health Technology and Informatics, Faculty of Health and Social Sciences, The Hong Kong Polytechnic University, Hong Kong Special Administrative Region
[c] Department of Neurosurgery, Taipei Veterans General Hospital, Taipei, Taiwan
[d] School of Medicine and Brain Research Center, National Yang-Ming University, Taipei, Taiwan
[e] School of Physical Therapy and Graduate Institute of Rehabilitation Science, Chang Gung University, Taoyuan, Taiwan
[f] Neuroscience Research Center, Chang Gung Memorial Hospital at Linkou, Taoyuan, Taiwan
[g] Department of Neurosurgery, Chang Gung Memorial Hospital at Linkou, Taoyuan, Taiwan
[h] Department of Neurology, Taipei Veterans General Hospital, Taipei, Taiwan
[i] Healthy Aging Research Center, Chang Gung University, Taoyuan, Taiwan

ARTICLE INFO

Article history:
Received 17 January 2019
Received in revised form
4 September 2019
Accepted 23 September 2019
Available online 24 September 2019

Keywords:
Focused ultrasound
Transcranial
Epilepsy
mTOR phosphorylation

ABSTRACT

Background: Epilepsy is a neurological disorder characterized by abnormal neuron discharge, and one-third of epilepsy patients suffer from drug-resistant epilepsy (DRE). The current management for DRE includes epileptogenic lesion resection, disconnection, and neuromodulation. Neuromodulation is achieved through invasive electrical stimulus including deep brain stimulation, vagus nerve stimulation, or responsive neurostimulation (RNS). As an alternative therapy, transcranial focused ultrasound (FUS) can transcranially and non-invasively modulate neuron activity.

Objective: This study seeks to verify the use of FUS pulsations to suppress spikes in an acute epileptic small-animal model, and to investigate possible biological mechanisms by which FUS pulsations interfere with epileptic neuronal activity.

Methods: The study used a total of 76 Sprague-Dawley rats. For the epilepsy model, rats were administered pentylenetetrazol (PTZ) to induce acute epileptic-like abnormal neuron discharges, followed by FUS exposure. Various ultrasound parameters were set to test the epilepsy-suppressing effect, while concurrently monitoring and analyzing electroencephalogram (EEG) signals. Animal behavior was monitored and histological examinations were conducted to evaluate the hazard posed by ultrasound exposure and the expression of neuronal activity markers. Western blotting was used to evaluate the correlation between FUS-induced epileptic suppression and the PI3K-mTOR signaling pathway.

Results: We observed that FUS pulsations effectively suppressed epileptic activity and observed EEG spectrum oscillations; the spike-suppressing effect depended on the selection of ultrasound parameters and highly correlated with FUS exposure level. Expression level changes of c-Fos and GAD65 were confirmed in the cortex and hippocampus, indicating that FUS pulsations deactivated excitatory cells and activated GABAergic terminals. No tissue damage, inflammatory response, or behavioral abnormalities were observed in rats treated with FUS under these exposure parameters. We also found that the FUS pulsations down-regulated the S6 phosphorylation and decreased pAKT expression.

Conclusion: Our results suggest that pulsed FUS exposure effectively suppresses epileptic spikes in an acute epilepsy animal model, and finds that ultrasound pulsation interferes with neuronal activity and affects the PTZ-induced PI3K-Akt-mTOR pathway, which might help explain the mechanism underlying ultrasound-related epileptic spike control.

* Corresponding author. Departments of Electrical Engineering, Chang-Gung University, Taoyuan, 333, Taiwan.
** Corresponding author. Graduate Institute of Rehabilitation Science, Chang Gung University, Taoyuan, Taiwan.
E-mail addresses: hsiehth@mail.cgu.edu.tw (T.-H. Hsieh), haoliliu@mail.cgu.edu.tw (H.-L. Liu).
[1] Sin-Guang Chen and Chih-Hung Tsai contributed equally to this study.

https://doi.org/10.1016/j.brs.2019.09.011

Introduction

Epilepsy is a common neurological disorder characterized by recurrent seizures, and is caused by brain injury or genetic factors involved in neuronal activities [1,2]. Epileptic seizures are typically sudden disturbances in brain function characterized by excessive and hyper-synchronous neural activity [3,4]. Epilepsy affects more than 50 million people worldwide [2,5] with an annual cumulative incidence of 68 per 100,000 persons [6]. Developing countries suffer a higher incidence rate than developed countries [5,6]. While over 20 medications have been developed for epilepsy, over one-third of epilepsy patients do not respond to any medication, a condition referred to as drug-resistant epilepsy (DRE) [2,7]. DRE treatment options include surgical resection or neuromodulation. Drug-resistant epilepsy patients with focal or regional onset can be treated with surgical resection to remove the epileptogenic area [8,9]. However, surgical resection is problematic when seizures are focused in the eloquent cortex (which governs language, motor skills, and visual senation). For these patients, brain neuromodulation is an alternative therapy to decrease the incidence of abnormal epileptogenic discharge [10].

Several noninvasive brain neuromodulation tools have been evaluated for the treatment of epilepsy [11,12]. The US FDA has approved neuromodulation devices which operate on the basis of deep brain stimulation (DBS), vagus nerve stimulation (VNS), and responsive neurostimulation (RNS) [9]. Other devices using transcranial magnetic stimulation (TMS) and transcranial direct current stimulation (tDCS) have been reported to provide noninvasive brain stimulation, but clinical trials have shown no benefit [13,14]. A primary limitation of TMS is that the inductive field decreases sharply and does not allow efficient energy deposition for subcortical stimulation [15]. Transcranial direct current stimulation (tDCS) has been proposed for seizure control by delivering weak direct current into the brain through electrodes [16]. However, the spatial resolution of tDCS energy is dispersed by the skull and suffers from short penetration distance [17].

Transcranial focused ultrasound (FUS) is a novel technique that allows energy to be precisely and noninvasively focused in deep brain tissue. The spatial resolution of low-intensity focused ultrasound is accurate to the order of millimeters and the penetration distance exceeds 10 cm, allowing brain tissue to be targeted through the intact skull [18,19]. Several studies have demonstrated that FUS can modulate brain neuronal activity in animal models [20,21] and can transiently manipulate transmembrane sodium or calcium channels [22,23]. Recently, FUS has been shown to decrease human motor cortical excitability [24]. The neuron modulation properties of FUS, especially the inhibition of neuronal excitability, may suppress hyperactivity of neuron during ictal onset. Min et al. previously showed that, under specific exposure conditions, FUS pulsations provide a suppressive effect on epileptic activation through electroencephalographic (EEG) assessment in a toxin-induced acute epilepsy model [25]. However, no systematic analysis of ultrasound exposure conditions has been completed for FUS epilepsy management, therefore the optimal selection of ultrasound parameters for this application has yet to be determined, and no investigation has been conducted to elucidate possible mechanisms for the suppressive effect of ultrasound stimulation on epilepsy.

The present study investigates the parametric selection of ultrasound exposure that provides epilepsy suppression. FUS pulsations were applied to PTZ-injected rats with different exposure levels, duty cycles, and exposure times to optimize the FUS anti-epileptic effect. Histological and behavioral tests were employed to confirm safety, and c-Fos and GAD65 expression change was immunohistologically tested to confirm neuronal and synaptic activity change. Previous studies have found that the linkage between seizure activation and the PI3K-Akt-mTOR pathway [26] is associated with seizure and epileptogenesis in animal models and humans [27,28]. Whether FUS pulsations affect the PI3K-Akt-mTOR pathway in PTZ-induced seizure rats was also evaluated.

Materials and methods

Experiment design

All animal experiments were approved by the Institutional Animal Care and Use Committee of Chang Gung University (IACUC No. 106–151). A total of 76 Sprague-Dawley rats (male, 276–300 g, BioLASCO Co., Ltd, Taiwan) were used. Among them, 36 rats were evaluated experimentally with EEG, 29 rats were chosen for behavioral testing and histology analysis to examine potential brain damage, 12 rats were examined by immunohistochemistry including GFAP, c-Fos and GAD65 expression level change, and 12 rats were examined by Western Blot.

Epileptic induction and EEG recording setup and analysis

Seizures were provoked in rats by intraperitoneal injection of PTZ (100 mg/kg, P6500, Merck KGaA, Darmstadt, Germany). EEG signals were recorded for 5 min as a baseline prior to PTZ administration, and for 30 min following PTZ administration (Fig. 2).

The EEG signal was amplified (1000x) and recorded (MP36, BIOPAC Systems Inc., Goleta, California, USA) at a sampling rate of 1000 Hz. The EEG signal was filtered using a band-pass infinite impulse response (IIR) filter operating between 20 and 100 Hz offline and subjected to software analysis (AcqKnowledge 4.2, BIOPAC Systems Inc., Goleta, California, USA). The epilepsy spikes were recognized as having an amplitude at least 7 times the standard deviation to the mean. Since the electrodes were positioned away from the incident sonication path as well as the sonication focus, and the ultrasound focal beam path did not penetrate through the electrode, thus the thermal effect can be eliminated.

Animal preparation and EEG setup

To investigate the effects of FUS on the PTZ-epilepsy model via EEG signals, 76 rats were divided into 6 groups with different acoustic levels (with at least six animals in each exposure group). Animals were anesthetized with urethane (1.2 g/kg, intraperitoneal injection). Before experimentation, we used the toe pinch response method to determine depth of anesthesia. All rats were unresponsive to the toe pinch before continuing. The rat scalps were dissected to expose the skull (Fig. 1B). Three burr holes were drilled to bilaterally implant four screw electrodes (1.6-mm-diameter pole; Plastics One Inc., Roanoke, Virginia, USA), and one reference electrode was used as a ground electrode using stereotactic coordinates. Cortical electrodes were placed epidurally (A = +2 mm, L = +2 mm for the frontal cortex; A = −8 mm, L = −4 mm for the parietal cortex; A = −10 mm, L = 0 mm for the ground electrode). Animals in group 1 were injected with PTZ without FUS sonication as a control to evaluate the EEG features of PTZ-epilepsy, where the other six groups conducted epilepsy onset using PTZ injection but followed varying FUS exposure levels (Table 1) to investigate the effects of FUS suppression on the PTZ-epilepsy mode. Prior to FUS exposure, the animal's scalp was shaved with clippers.

EEG signals were acquired with two cortical stainless steel screw electrodes (1.6-mm-diameter pole; E363, Plastics One Inc., USA) with a ground electrode contact positioned over the lambda of the skull (Fig. 1B). The EMG signal was amplified (gain = 2000) and filtered using a 60-Hz notch prior to digitization at 1 kHz

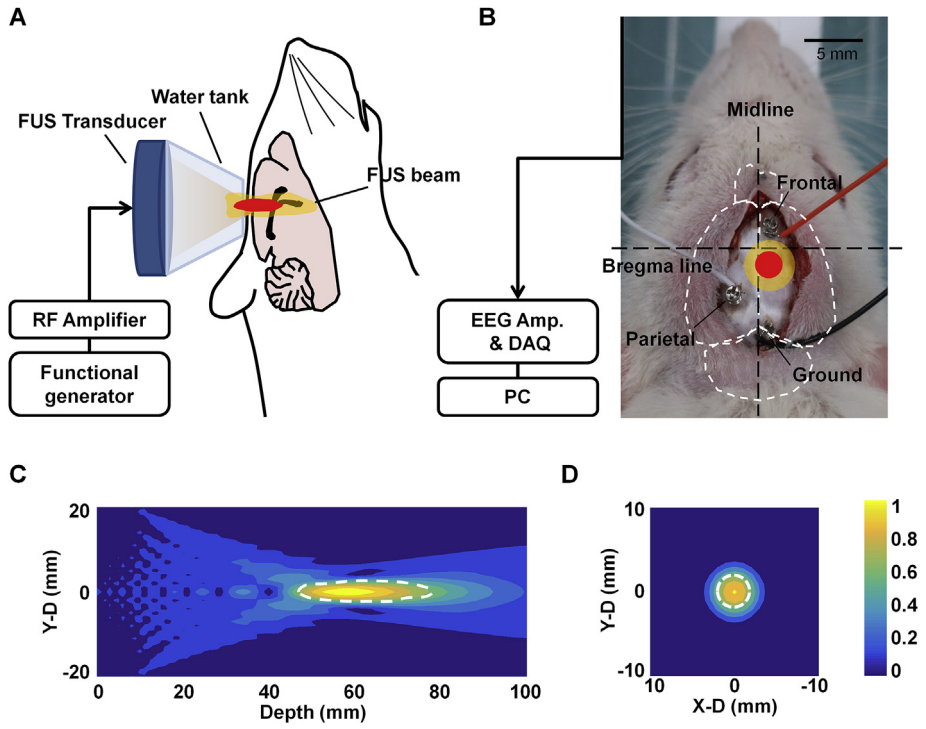

Fig. 1. Conceptual schematic of the experimental setup and topographical sonication depth. (A) The transducer was used on a 3-axis dimension system. The transducer was immersed in degassed water. The focused ultrasound setup for epilepsy therapy is described in the Materials and Methods section. (B) The schematic diagram illustrates the relative positions of the EEG electrodes and focused ultrasound (FUS) beam on the rat skull. (C and D) The relative depth and distance of FUS were detected under the rat skull. Dashed contours outlines -3dB pressure distributions.

(MP36, BIOPAC System, California, USA). Epileptic spikes were counted by optimizing the automated seizure detection algorithm in AcqKnowledge 4.2 (BIOPAC System, California, USA) in each time window (spikes/5 min) in rats injected with PTZ and treated with or without focused ultrasound. Spikes were defined as a sharp deflection with amplitude $\geq 2\times$ the background activity lasting 40–60 ms in duration [29]. Furthermore, for the analysis of the epileptic spike burst, a blinded reviewer checked single

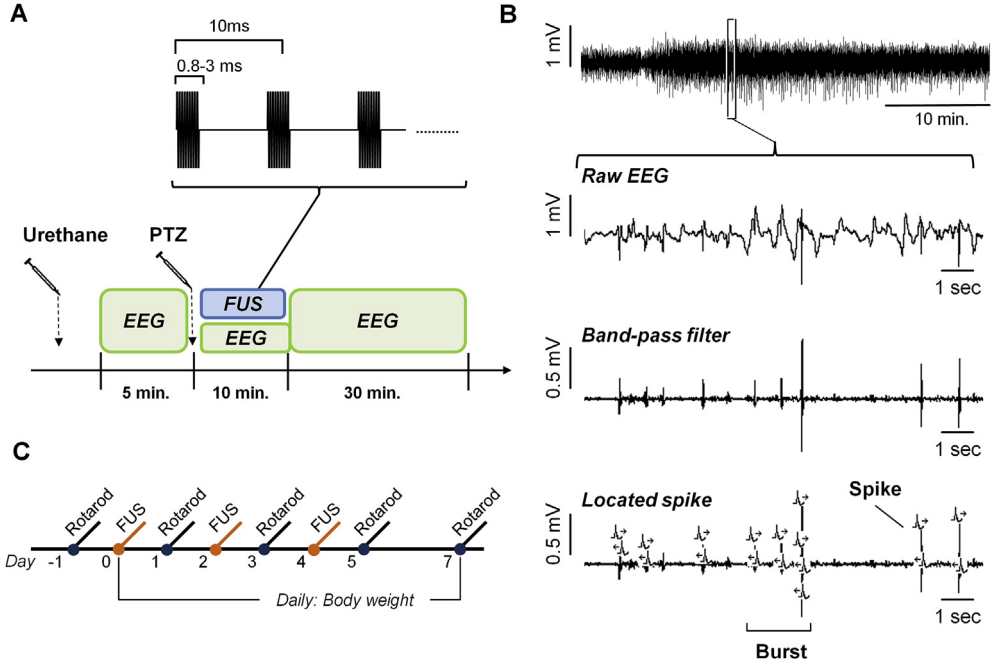

Fig. 2. Flowchart of the EEG recording and schedule of behavior examination. (A) The EEG signal was recorded for 5 min prior to PTZ injection, for 10 min following PTZ injection, and for 20 min following FUS treatment. (B) The raw EEG signal was recorded and a band-pass filter was used to identify spikes. (C) The behavior test was executed according the schedule to determine whether FUS treatment affects rat performance on the rotarod assay.

Table 1
Summary of acoustic parameters used in individual experimental groups. MI = Mechanical index, DC = duty cycle, t = total exposure time, I_{spta} = spatial-peak temporal-averaged intensity, I_{sptp} = spatial-peak temporal-peak intensity. FUS energy deposited in the brain with respect to intensity I_{spta} and I_{sptp} respectively denoted as $I_{spta} \times t$ and $I_{sptp} \times t$.

Level	MI	DC (%)	t (sec)	I_{spta}(W/cm^2)	I_{sptp} (W/cm^2)	$I_{spta} \times t$(J)	$I_{sptp} \times t$ (J)	Animal number (n)
0	0	0	0	0	0	0	0	20[a,b,c,d,e]
1	0.375	30	600	0.703	2.34	422	1404	6
2	0.75	8	600	0.75	9.38	450	5628	15[b,d]
3	0.5	30	600	1.25	4.17	750	2502	6
4	0.75	30	100	2.812	9.37	281	937	7[a]
5	0.75	30	600	2.812	9.37	1687	5622	22[a,b,c,d,e]

[a] Hematoxylin and eosin (HE) staining was conducted in partial brain samples (n = 4).
[b] GFAP immunohistochemistry staining was conducted in partial brain samples (n = 4).
[c] C-Fos and GAD65 immunohistochemistry staining were conducted in partial brain samples (n = 8).
[d] Rotarod testing was conducted in partial animals (n = 29).
[e] S6 and Akt expression changes via Western blot testing were conducted in partial animal brain samples (n = 12).

epileptiform spikes as well as spike trains. A pattern of repetitive epileptic spikes (≥3 continuous spikes) lasting at least 1 s was categorized as a burst [30]. For further analysis of oscillation of EEG following FUS intervention under PTZ-induced epilepsy, spectral analysis was applied to the EEG. The power spectral density (PSD) with a total 5-min EEG duration was computed via fast-Fourier transform, with PSD analyzed either in total spectrum (1–100 Hz) or band selection including alpha (8–13 Hz), beta (13–30 Hz), theta (4–8 Hz), gamma (40–100 Hz). The values of mean PSD power and spectrum median frequency in each band were calculated.

Focused ultrasound calibration

A spherical focused ultrasound transducer (SonicConcept, U.S; fundamental frequency = 0.5 MHz, radius curvature = 64.3 mm; diameter = 64.3 mm) was used. For ultrasound energy exposure, RF signals of 0.5 MHz were generated by a function generator (A33420, Agilent, USA) and amplified by a radiofrequency power amplifier (240L, E&I, USA). The acoustic pressure field was measured in a free field within an acrylic tank filled with deionized/degassed water by a moving needle hydrophone (HNA-0400, ONDA Corp., Sunnyvale, California, USA) positioned on a stepping-motor controlled 3-D positioning system, with steps of 1 mm. The fields of view in the axial and cross sections were respectively 40 × 100 mm and 40 × 40 mm. The diameter and length of the half-maximum pressure amplitude of the ultrasound field were respectively 2 and 12 mm (Fig. 1C and D). The FUS trajectory traveled through the cortex, hippocampus and thalamus regions (Fig. 1B) when coordinating this FUS energy deposition region to the rat brain atlas [31].

In-vivo ultrasound experiments

For small-animal ultrasound exposure experiments, the FUS transducer was submerged in a custom-designed acrylic water tank (Fig. 1A). The peak negative pressure exposure (P) at focus ranged from 0 to 0.53 MPa (free-field measured pressure level after considering 10% transcranial pressure loss), which are respectively equivalent to a mechanical index (MI) of 0–0.75. The exposure parameters were fixed at a pulse repetition frequency of 100 Hz and the total exposure time (t) was either 100 or 600 s, but the duty cycle (DC) was set either 8 or 30%. FUS exposure intensity (denoted as I) was defined either as spatial-peak temporal average (denoted as I_{spta}, where $I_{spta} = \mathrm{DC} \times P^2/2\rho c$, ρ is density and c is sound speed), and a spatial-peak temporal-peak (denoted as I_{sptp}, where $I_{sptp} = P^2/2\rho c$). The acoustic levels used during the experiment are summarized in Table 1. The spike numbers of EEG bursts were calculated using Biopac Student Lab (Upwards Biosystems, Taiwan) in each time window (spikes/5 min) in rats injected with PTZ and treated with or without focused ultrasound.

Behavioral monitoring

The behavioral test examined potential brain damage caused by repeated sonication. Eighteen rats were divided into 3 groups, (acoustic levels 0, 3, and 5), to evaluate the behavioral effect via Rota-Rod (LE8305, Panlab S. L., Havord Apparatus, Spain; revolutions-per-minute (rpm) set to 15 on Days 0, 1, 3, 5, and 7; FUS exposure conducted on Days 0, 2, and 4 (Fig. 2C).

Histological analysis

For hematoxylin Eosin (H&E) staining, brain sections were deparaffinized with xylene and rehydrated with 100%, 95%, and 70% ethanol (n = 4). The sections were stained with hematoxylin, washed with tap water, differentiated in 1% alcohol, saturated lithium carbonate, and stained with eosin. Under microscope observation, the nuclei should be blue and the cytoplasm should be pink. To identify changes in neuronal and synaptic activity following FUS pulsations, the molecular marker glial fibrillary acidic protein (GFAP), c-Fos and GAD65 were used to analyze expression level change in the cortex, hippocampus and thalamus for immunohistochemical (IHC) methods (n = 8). Briefly, rat brains were post-fixed in a 4% paraformaldehyde fixative solution (PFA) and cytoprotected in 30% sucrose solution for 48 h at 4 °C. The cerebral tissues were sectioned into coronal blocks with a thickness of 30 μm on a cryostat (Leica CM3050 S Cryostat, FL, US), and sections containing hippocampus thalamus were quenched with 0.3% H_2O_2/PBS for 10 min, 10% milk (Anchor Shape-up, New Zealand) for 1 h to block non-specific antibody and then incubated with primary rabbit polyclonal anti-GFAP antibody (1:4000, N1506, Agilent Technology, USA), anti-c-fos (1:1000, AB190289, abcam) or anti-GAD65 (1:100, GAD65-101AP, FabGennix) for 1 h at room temperature. After washing with PBS for three times, the sections were incubated with secondary anti-rabbit antibody (1:200, MP-7401, Vector Labs, USA) for 1 h at room temperature. The sections were finally developed using a solution of 3, 3-diaminobenzidine (DAB, SK-4105, Vector Labs, USA) for 3–5 min.Sections were then mounted on slides, allowed to dry and dehydrated with graded alcohols, cleared with xylol (Sinopharm, China), cleared in xylene and cover-slipped in DPX. The number of c-fos positive or GAD65 positive cells were analyzed using Image-J software (Media Cybernetics, USA).

Western blotting

The other set of animals was sacrificed by decapitation after different treatments (n = 12). Cortex and hippocampus tissue was harvested and immediately frozen in liquid nitrogen for storage at −80 °C before analysis. Frozen tissues were immersed in RIPA solution (10 μl/mg, TAAR-ZBZ5, Biotools Co., Ltd. Taiwan), and supernatants were collected. The protein concentration of supernatants was determined using a Bio-Rad protein assay kit (5000001, Bio-Rad Laboratory Inc., Hercules, CA, USA). Tissue lysate was separated by SDS-PAGE (GL2510, SMOBIO Technology Inc., Taiwan) and transferred to polyvinylidene fluoride (PVDF) membrane (1620177, Bio-Rad Laboratory Inc., Hercules, CA, USA). After washing in Tris-buffered saline (TEB-BTBS1L, Biotools Co., Ltd. Taiwan) containing 0.05% Tween-20 (TBS-T), the blots were blocked with 5% non-fat milk dissolved in TBS-T at room temperature for 1 h and incubated at 4 °C overnight with the following primary antibodies: mouse anti-Akt (1:2000, #2920, Cell Signaling Technology, USA); rabbit anti-S6 ribosomal protein (1:1000, #2217, Cell Signaling Technology, USA); rabbit anti-phospho-Akt (Ser473) (1:1000, #4060, Cell Signaling Technology, USA); and rabbit anti-β-actin (1:2000, A2103, Merck KGaA, Darmstadt, Germany). The membranes were thrice washed with TBS-T and probed at room temperature for 1 h with horseradish peroxidase (HRP) conjugated (1:2000, A0545, Merck KGaA, Darmstadt, Germany) goat anti-rabbit IgG, or mouse IgG kappa binding protein conjugated to HRP (1:2000, sc-516102, Santa Cruz Biotechnology, USA). The signal of HRP was rendered visible with immobilon western chemiluminescent HRP substrate (WBKLS0500, Merck KGaA, Darmstadt, Germany) and detected using a chemiluminescence imager (Amersham Imager 600, GE Healthcare Life Sciences). The band intensity was quantified by ImageJ software.

Statistical analyses

Results are displayed as means ± SD. Most statistical analyses were calculated by Graphpad Prism 5 software (GraphPad Software Inc., San Diego, California, USA). Tukey post-hoc tests were computed by Graphpad Prism 8 software (GraphPad Software Inc., San Diego, California, USA). Two tailed unpaired Student's t-test was used to compare the mean values of the two groups. Two-way ANOVA was used to compare the spike number, bursts and EEG power spectrum between PTZ-induced rats treated with or without FUS. To fully understand group differences in an ANOVA, Tukey post-hoc tests were used. Tukey's multiple comparison analysis method compared each experimental group to each control group. A p value less than 0.05 or 0.001 is considered significant.

Results

Epileptic onset regulated by FUS exposure

Fig. 3 shows representative EEG data collected from animals following various levels of FUS exposure, showing both unfiltered EEG signals and extracted theta waves. Prior to PTZ injection no unusual EEG signal bursts were apparent, but epileptic EEG signal bursts were detected from 10 min following PTZ injection. During FUS treatment, the number of EEG bursts in rats treated with FUS pulsations clearly decreased following sonication, showing that the occurrence of atypical spikes induced by PTZ-injection can be repressed by FUS pulsations.

Fig. 4 provides a detailed comparison of the PTZ-induced theta burst numbers in the various treatment groups.

The EEG signals in all FUS-treated groups all showed significant decrease in the number of spikes when compared with the untreated groups (acoustic level 0) at 10–15 min after PTZ injection. However, at 15–20 min duration, only the acoustic level 2 (0.75-MI, 8%, 600s) and acoustic level 5 (0.75-MI, 30%, 600s) groups presented significant a spike suppression effect, while the other FUS-treated group did not show a statistical difference in the number of spikes compared with the untreated group. The number of abnormal theta bursts decreased from 45 ± 16.971 (n = 6) in the untreated group to 7.714 ± 9.517 (n = 6; $p < 0.001$) in the level-2 group or 5.400 ± 5.771 (n = 6, $p < 0.001$) in the level-5 group. In Tukey's multiple comparison test, the F-value of time was 18.45 (F (DFn, Dfd) = F (2.654, 82.28) = 18.45) and its p-value was less than 0.0001 for acoustic level-2 group, whereas the F-value of treatment was 6.329 (F (DFn, Dfd) = F (6, 31) = 6.329) and the p-value was equal to 0.0002 in acoustic level-5 group.

In addition, a 5-min period of EEG recording post-PTZ was digitally scored to quantitate the epileptic bursts. Fig. S1 shows the changes in spike burst count after PTZ injection with different FUS levels. The burst count of acoustic levels 2, 3 and 5 was significantly less than in sham-stimulated animals (acoustic level 0; $p < 0.05$). Fig. 5A shows the representative PSDs at pre- and post-PTZ administration (during 10–15 min period; acoustic levels 0 and 5), demonstrating that FUS pulsations significantly suppressed PSD levels during epileptic onset (Fig. 5B and S2; from $(1.45 \pm 2.34) \times 10^{-9}$ to $(4.55 \pm 1.24) \times 10^{-9}$ mV^2/Hz in acoustic levels 0 and 5, respectively), and resulted in a noticeable median frequency shift (Fig. S2; from 90.13 ± 6.55 to 68.57 ± 7.98 Hz in levels 0 and 5, respectively). Additional analysis of potential frequency in gamma band (Fig. 5C) and other band frequencies (Fig. S2) showed that the gamma band (40–100 Hz) increased due to PTZ administration, and the intervention of FUS pulsations (particularly in acoustic levels 2, 4, and 5) effectively inhibited PSD levels in gamma ($p < 0.05$). FUS pulsations also demonstrated suppressive effects in the alpha, beta and theta bands, particularly in acoustic level 4 and 5 conditions.

Histological examination of brain injuries and behavior testing

FUS pulsations may induce neuron damage, thus mitigating abnormal EEG burst due to PTZ. To rule out this possibility, rats were treated with or without FUS pulsation and sacrificed 24 h later. No obvious adverse reaction was observed in rats treated with acoustic level 6 exposure over 24 h. Following deep anesthesia, perfusion was performed with normal saline and the rats' brains were dissected, fixed in 10% neutralized formalin, embedded in paraffin, sectioned to 4-μm thick slides and stained with hematoxylin and eosin. Coronal sections of brains from FUS-treated and naïve animals were assessed for tissue damage (Fig. 6). Low-magnification images revealed no obvious tissue disruption regardless of FUS pulsation. High magnification H&E images showed no immune cell infiltration or microglia activation and expansion around the cortex or hippocampus area. These findings demonstrate that FUS does not cause damage or inflammation in rat brains.

In addition, immunohistochemistry staining using an anti-GFAP antibody as well as H&E staining both showed no obvious evidence of astrogliosis at or near the sonicated sites in brains treated with FUS compared against naïve animals (Figs. 7 and 8). No high astrocyte density region or enlarged astrocyte bodies were found in the brains of FUS treated rats. Furthermore, we observed histological change in the brains of rats at 1, 3, and 7 days following FUS pulsation using anti-GFAP staining, and the results for rats treated with FUS were similar to those of naïve animals. These findings indicate that FUS treatment does not affect the normal phenotype of astrocytes in rat brains.

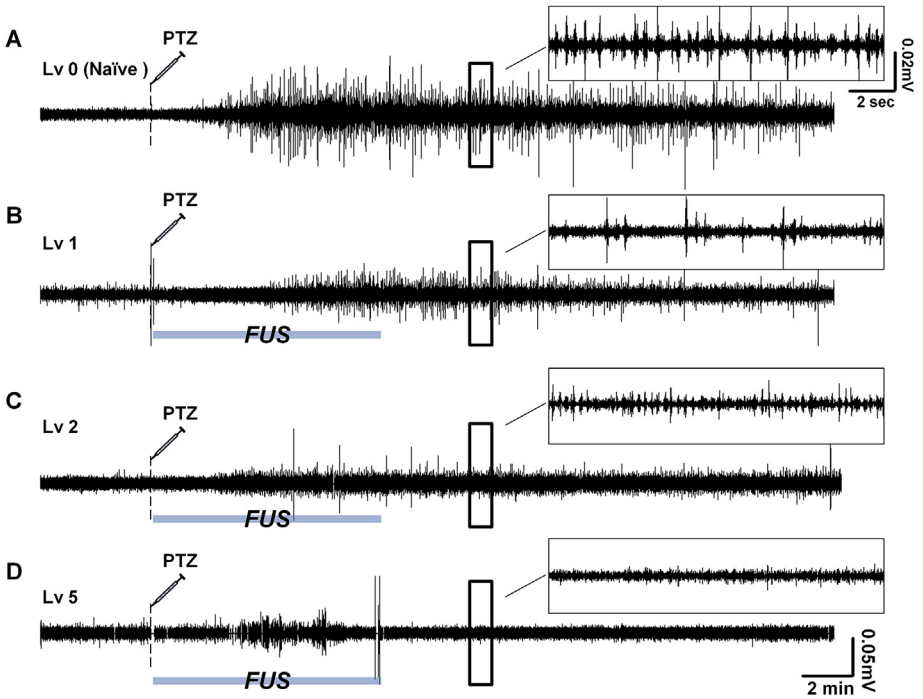

Fig. 3. Electroencephalographic (EEG) recordings from PTZ-injected rats and FUS treated rats displayed in a time-course manner. The representative EEG recordings from PTZ-injected rats (A; acoustic level 0) and PTZ-injected rats treated with 0.375 MI, 30% duty cycle (B; acoustic level 1), 0.75 MI, 8% duty cycle (C; acoustic level 2), and 0.75 MI, 30% duty cycle (D; acoustic level 5).

We further verified the expression of c-Fos and GAD65 as a marker of neuronal and synaptic activity after FUS treatment. The changes in marker protein expression in c-Fos and GAD65 on animal brains were demonstrated either in FUS (acoustic level 5) and naïve animal (acoustic level 0) measured from cortex, hippocampus and thalamus (Fig. 8 and S3). Animals receiving FUS pulsations showed significant increases in c-Fos-positive neurons either in the cortex ($t = 3.61$, $p = 0.036$) and hippocampus ($t = 3.90$, $p = 0.029$) but no significant difference was found in the thalamus ($t = 1.87$, $p = 0.159$) when compared to the non-FUS hemisphere. In GAD65 analysis, FUS pulsations strongly increased the number of GAD65-positive cells in the cortex compared with non-FUS treated hemisphere ($t = 4.10$, $p = 0.026$); however, no significant difference was shown in the hippocampus ($t = 1.86$, $p = 0.159$) and thalamus ($t = 1.39$, $p = 0.26$) when compared between each hemisphere. As to sham-FUS animals, no significant difference was observed when compared with two hemispheres (all $p > 0.05$).

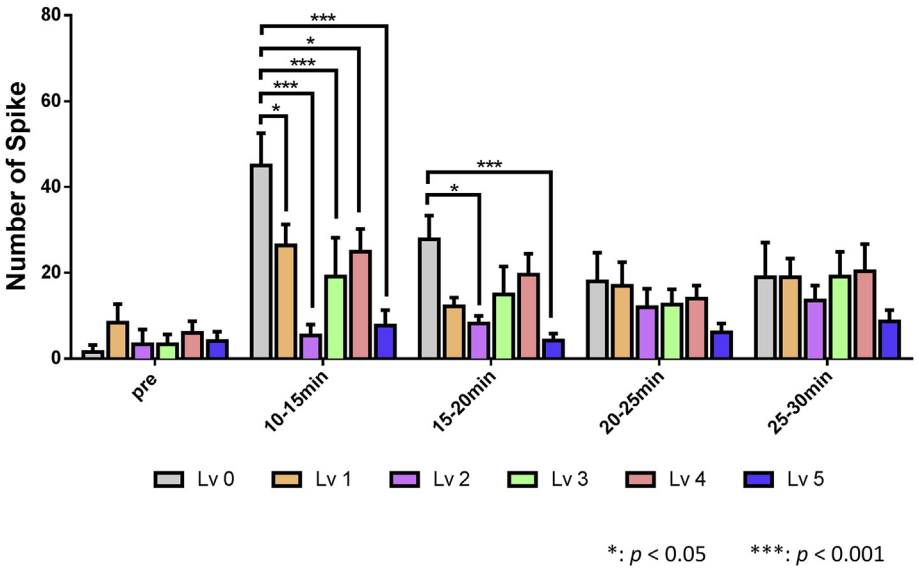

Fig. 4. Quantification of epileptic EEG signal spikes under varying FUS exposure conditions. The number of epileptic EEG spikes in different time frames was calculated from raw EEG peaks in groups of PTZ-injected rats and PTZ-induced rats treated with different FUS intensity levels. The bar chart compares EEG bursts in PTZ-induced rats treated with or without FUS in different time frames. The results are means ± SE of seven animal groups. *: $p < 0.05$, ***: $p < 0.001$.

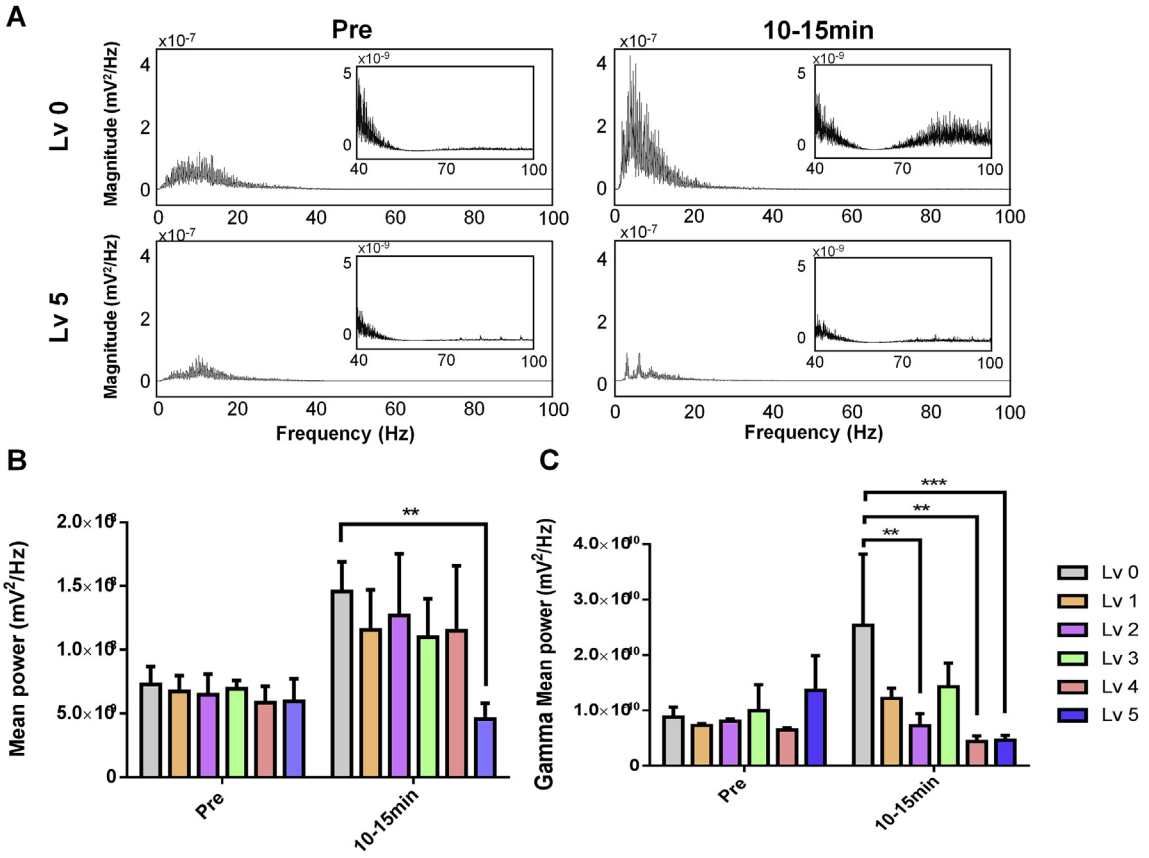

Fig. 5. (A) Comparison of power spectral density (PSD) changes between pre- and post-PTZ (10–15 min duration) administration in naïve (level 0) and FUS-treated (level 5) animals. Zoomed subplots represent gamma band highlights. (B) Comparison of mean PSD level throughout the entire spectrum among all acoustic-level groups. (C) Comparison of mean PSD level at gamma band among all acoustic-level groups.

To investigate whether FUS pulsation influences the motor coordination of rodents, we performed a rotarod performance test to evaluate the cerebellar function in FUS-treated rats. No significant difference in rotarod performance was found between untreated rats and rats treated with 0.75-MI FUS pulsation, 8% or 30% duty cycle, 600 s at 1, 3, 5, and 7 days following FUS treatment (i.e., level 2 and 5, respectively; Fig. 9A). During the rotarod performance test, rats were observed daily for change in body weight, but no significant decrease in body weight was found in any group (Fig. 9B), suggesting that FUS pulsation is safe and does not cause brain malfunction in rats.

Western blot examination

PTZ is known to induce mTOR pathway activation in rat brains. Ultrasound stimulation in the osteoblast activates the mTOR pathway [32]. Attenuation of mTOR pathway activity suppresses PTZ-induced acute status epilepticus in rats [33]. This raises the possibility that FUS pulsation affects PTZ-induced mTOR pathway activation. We examined the downstream target of the mTOR pathway, the phosphorylation of S6, in the cortex and hippocampus of rats following PTZ injection and FUS treatment by western blot assay. Rats were injected with or without PTZ and treated with or

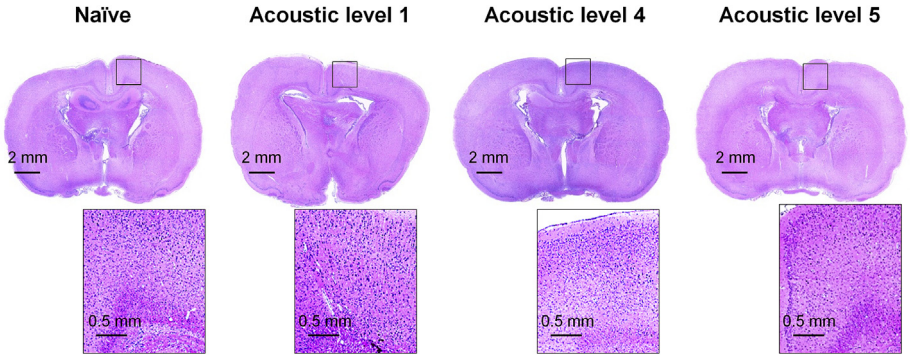

Fig. 6. Histological examination of brain injury. Comparison of hematoxylin and eosin staining in brain sections obtained from naive and FUS treated rats was carried out. These histological results were similar for naive (FUS-) and FUS treated brain sections (acoustic levels 1, 4, and 5). The large rectangles show a higher magnification of the cortex and hippocampus sections.

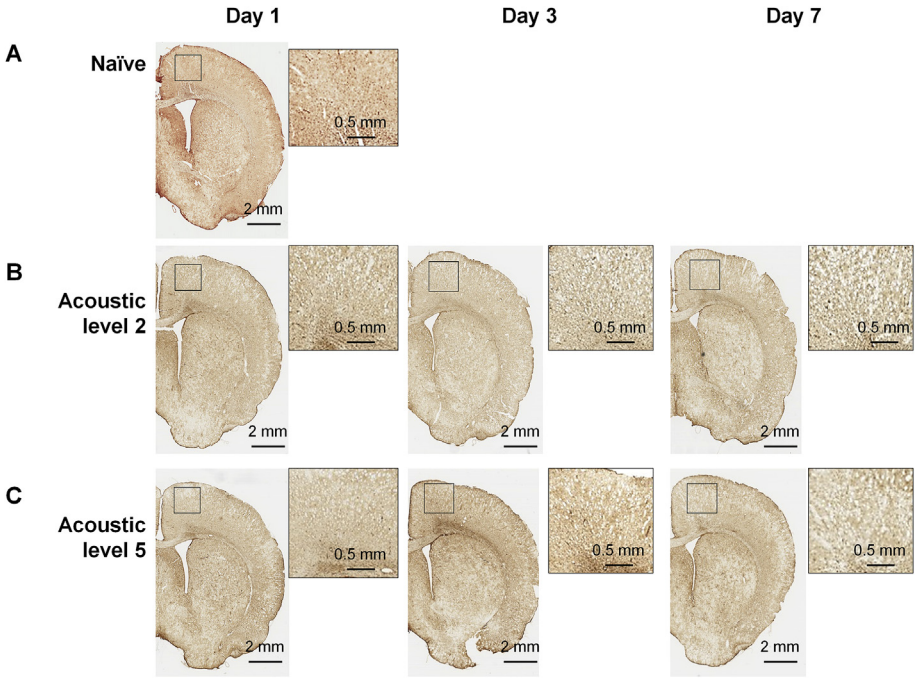

Fig. 7. Results of GFAP immunohistochemistry on rat brain sections from naïve rats (A), rats treated with acoustic level 2 (B), and rats treated with acoustic level 5 (C) stained with anti-GFAP antibodies. The brain samples in the FUS treated group were collected 1, 3, and 7 days after sonication treatment. The large rectangles show a higher magnification of the cortex and hippocampus sections.

without FUS pulsation (acoustic level 5; 0.75 MI, 30% duty cycle, 600 s). The right and left cortices were collected from the rat brain section 15 min after PTZ injection. Tissue protein was subjected to western blotting with antibodies to phosphorylated S6, S6, and β-actin. Comparing the ratios of p-S6 to S6 in the cortex of PTZ-injected rats with control animals, the ratios in the PTZ group were increased (Fig. 10A). Furthermore, FUS treatment attenuated these increases, as evidenced by statistical differences among the ratios between the PTZ and the FUS + PTZ groups ($p < 0.01$, Fig. 10A). A similar pattern was observed for the hippocampus region but no statistical difference was found between the PTZ and the FUS + PTZ groups (Fig. 10B). These findings verify that mTOR is activated by PTZ and FUS-pulsation attenuates the activation of mTOR.

Next, we determined whether FUS treatment would affect Akt/mTOR/s6 cascade in PTZ-stimulated rats. The phosphorylation of Akt at Ser473 was examined in the cortex of rats subjected to PTZ injection and FUS treatment by western blotting. The PTZ-stimulated phosphorylation of Akt at Ser473 in the right cortex was alleviated by FUS pulsation compared against PTZ-injected rats (Fig. 10C). These findings suggest that FUS pulsation suppresses the PTZ stimulated Akt/mTOR/s6 signaling pathway.

Discussion

This study demonstrates that focused ultrasound pulsation effectively suppresses acute epileptic neuron activity in a PTZ-induced acute epilepsy animal model. This is the first parametric investigation of ultrasound parameters in optimizing epilepsy suppression. We observed that FUS exposure with exposure levels reaching 0.75-MI with exposure time of 600s provided an effective spike-suppressing effect.

In this study, we have selected various combinations of ultrasound parameters to select effective FUS exposure conditions to suppress epilepsy-like spikes. Our results show that low-intensity FUS pulsation can effectively suppress the number of EEG bursts in rats with PTZ-induced acute epilepsy; however, the suppressive effect significantly depends on the selection of ultrasonic parameters. To evaluate the impact of the duty cycle, we compared level 2 (8%) and level 5 (30%) when fixing the other parameters to 0.75-MI/600s, and we did not see an impact of the duty cycle. To evaluate the impact of the exposure pressure level, we compared results obtained from levels 1 (0.375-MI), 3 (0.5-MI), and 5 (0.75-MI) when fixing the other parameters to 30%/600s, finding a high correlation with spike-suppression effect ($r^2 = 0.945$; see Fig. S3). To evaluate the influence of exposure time, we compared results obtained from level 4 (100s) and level 5 (600s) while fixing the other parameters to 0.75-MI/30%, and observed a significant impact on the spike-suppressing effect. Since both exposure pressure level and exposure time seemed to be correlated with the spike-suppressing effect, we therefore evaluated the correlation with spatial-peak temporal-peak fashioned energy (i.e., $I_{sptp} \times t$), finding a high correlation ($r^2 = 0.782$; see Fig. S3). We also evaluated the correlation with spatial-peak temporal-average intensity (I_{spta}) and spatial-peak temporal-averaged fashioned energy (i.e., $I_{spta} \times t$). However, Neither I_{spta} nor $I_{spta} \times t$ provided sufficiently high correlation with the spike-suppressing effect ($r^2 = 0.279$ and 0.435, respectively; see Fig. S3). Overall, we determined that ultrasound exposure level (MI) should serve as a critical contributor to the spike-suppressing effect, whereas the other parameters also interfered with the epilepsy-modulating effect and serve as supporting factors.

Focused ultrasound has been previously shown to have therapeutic potential for epilepsy control. King et al. provided a systemic investigation in a preclinical small animal setup to find that ultrasound intensity levels of 1–10 W/cm^2 are required to provide a sustainable and reproducible neuro-stimulation effect [34]. Aside from the exposure pressure level, previous preclinical studies have found that ultrasound neuromodulation is highly dependent on frequency selection, with an ultrasound center resonance frequency of < 0.5 MHz providing sufficiently high yield and an

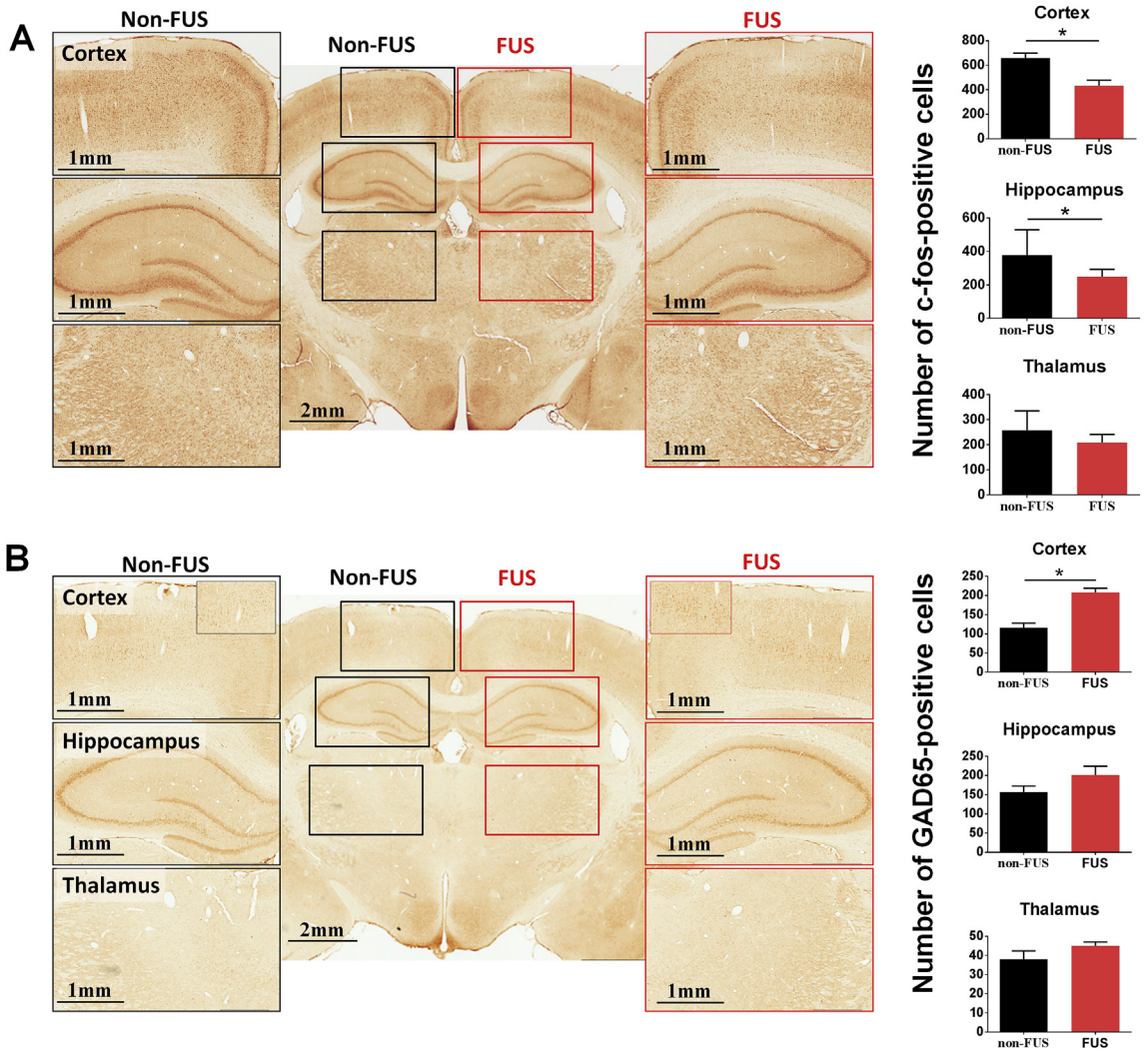

Fig. 8. (A, B) c-Fos and GAD-65 immunohistochemistry of rat brain sections. Brain sections were obtained from rats treated with acoustic level 5 (0.75 MI, 30% duty cycle, 600 s). Brain sections were stained with anti-c-Fos antibodies. Cortex regions displayed with higher magnification are also shown to compare the untreated (black box) and FUS treated (red box) sites. (For interpretation of the references to colour in this figure legend, the reader is referred to the Web version of this article.)

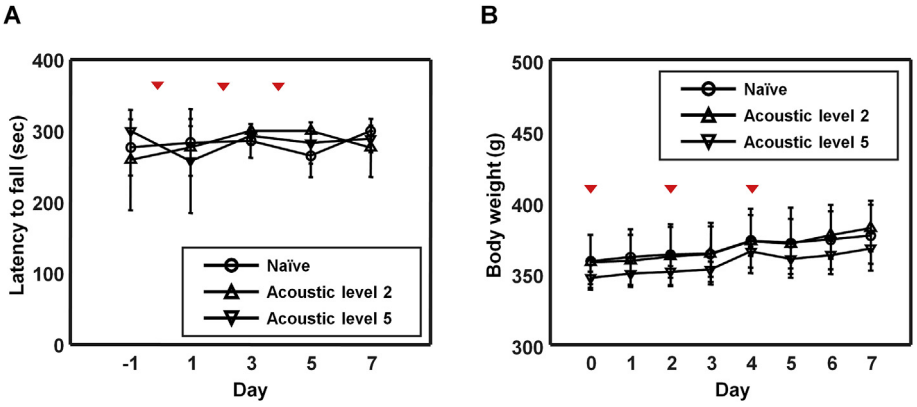

Fig. 9. The performance of rotarod assay and physiological states in rats treated without or with FUS was monitored daily after FUS treatment. (A) Rotarod assay was used to evaluate rat motor skill by recording fall latency. Data are represented as mean ± SD (n = 6 per group). (B) The body weight of rats was recorded daily to assess physiological state following FUS treatment. Data are mean ± SD of six rats.

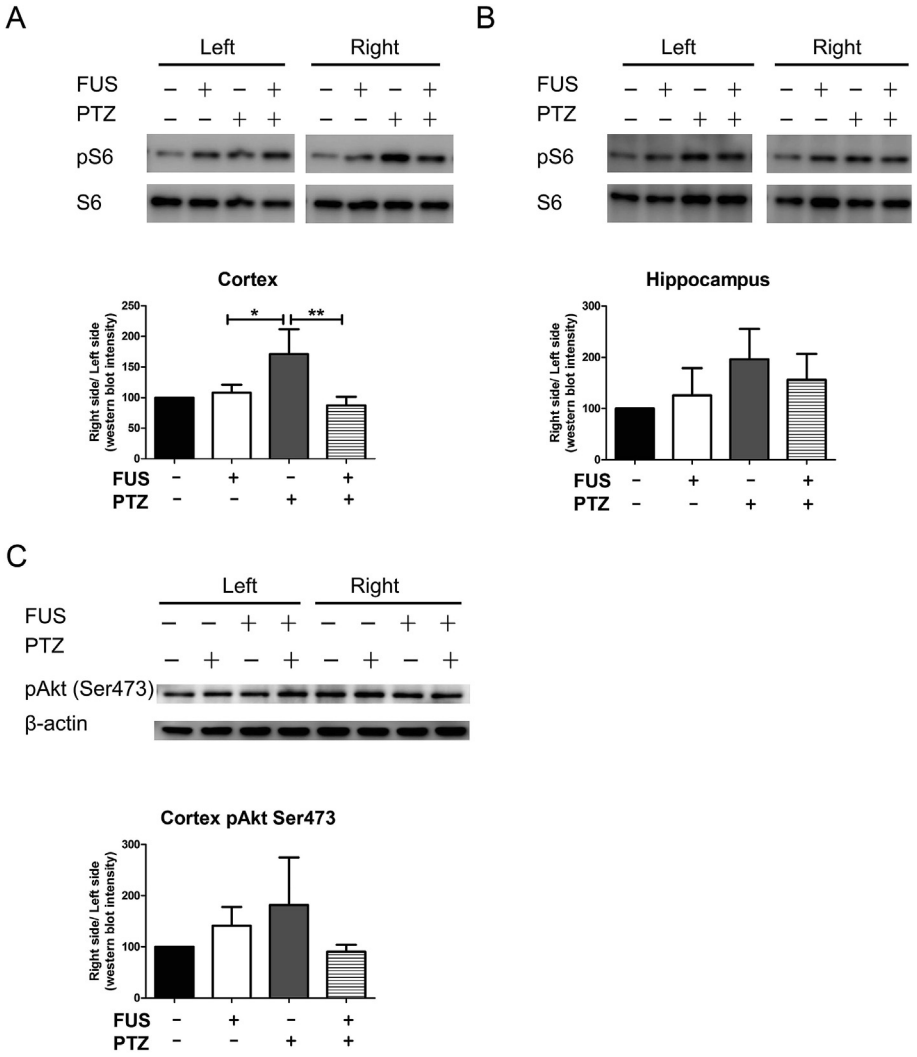

Fig. 10. FUS treatment suppressed the PTZ-induced hyper-phosphorylation of S6 and Akt at Ser473 in the right hemisphere, with the left brain hemisphere serving as control. Animals were treated with acoustic level 5 (0.75 MI, 30% duty cycle, 600 s). (A) The phosphorylated S6 and S6 detected by western blotting with cortex tissue. (B) The phosphorylated S6 and S6 detected by western blotting with hippocampus tissue. (C) The expression of phosphorylated Akt at Ser473 and β-actin with cortex tissue.

exposure level-dependent neuro-stimulation effect [35]. In 1964, Manlapaz et al. first described the use of focused ultrasound to suppress chemical-induced (i.e., direct brain injection of alumina cream) local epilepsy in cats [36]. The underlying mechanism contributes to a thermal effect, since the ultrasound intensity of 840 W/cm^2 caused permanent thermally necrotic brain damage. Yoo et al. and Hakimova et al. both described the use of non-thermal ultrasound pulsations to stimulate chemical-toxin (administration of kainate or PTZ) induced epilepsy, and also concluded that ultrasound pulsations can suppress epileptic activity [25,37]. These two studies both applied low burst ultrasound intensity (0.13–0.16 W/cm^2) and showed sustained or, in some indexes, significant epileptic activity suppression. Although no specific biochemical evidence is provided, these two studies both suspect that the activity of voltage-gated Ca^{2+} or Na^{+} ion-channels on the membrane can be influenced [22], leading to the concentration of transmembrane ions or altering neurotransmitters, thus contributing to the regulation of neural activity. The exposure level selection is comparable with that used in current clinical applications reported to provide tactile sensation, EEG peak/latency change, or inhibition of motor-evoked potentials (Fomenko, 2018; MI = 0.3–1.1, I_{spta} = 3–6.16 W/cm^2 [38]). A recently launched clinical trial has also attempted to use transcranial focused ultrasound pulsation to suppress epilepsy (clinical identifier NCT03657056; MI = 0.3, I_{spta} = 0.72–5.76 W/cm^2).

The strong decrease in c-Fos and increase GAD65 expression signals a strong deactivation of excitatory neurons and activation of inhibitory synapses. A strengthening of the GABAergic synapses by FUS is supported by another non-invasive approach in an rTMS animal study finding of increased GAD65 expression following cTBS [39], which is indicative of enhanced presynaptic GABA-synthesis. Expression of GAD65 is predominant in the GABAergic synapse for tonic inhibition and GAD65 has been reported as being critical for the synthesis of GABA destined for extrasynaptic tonic inhibition for regulating epileptiform activity [40]. These data indicate that FUS pulsations can drive neural excitatory (c-Fos, activation of cells) and inhibitory (GAD65) synaptic transmission. With regard to our findings, we postulate that increased GAD65 expression and reduced c-Fos expression indicates that the neural network is augmented by the given FUS pulsation parameters in an inhibitory fashion, and may serve as evidence that FUS pulsations have the potential to suppress epileptiform activity.

This study also reports that the spike-suppressing effect is correlated with down-regulated PTZ-induced S6 phosphorylation

and Akt phosphorylation. PTZ is a GABA-A receptor antagonist that has been shown to mimic acute stage neuronal activity during the onset of clinical epilepsy [41], and the same mechanism could potentially be used for clinical treatment of epilepsy. Zhang and Wong demonstrated that PTZ injection activates the mTOR pathway in both the hippocampus and neocortex of rats [26]. Aberrant dysregulated mTOR activity has been implied in enhancing epileptogenesis in several types of epilepsy and is a target for the development of anti-epileptic drugs [7,42,43]. Focused ultrasound-mediated disruption of the Blood Brain Barrier is associated with the activation of Akt in neuronal cells of sonicated rat brain regions [44]. Ultrasound induces the activation of integrin $\alpha_5\beta_1$/integrin-linked kinase/Akt/mTOR pathways in osteoblasts [32]. Both Akt and protein phosphatase 2A (PP2A) are associated with β_1-integrin-organized cytoplasmic complexes and PP2A displays higher levels of activity in the complexes [45]. PP2A can remove phosphate groups from Akt and deactivate Akt. Ivaska et al. demonstrated that an integrin can deactivate Akt by affecting PP2A [46].

In addition, ultrasound related S6/Akt phosphorylation also links with ion-channel membrane regulation to our confirmed pathway, as previous studies have also demonstrated that the expression of Kv1.1, Kv1.2 and Kvβ2 voltage-gated potassium channels are repressed by mTOR [47,48]. The expression of potassium channels ensures that the membrane potential reconstitutes to the neuron resting state. In summary, it might be possible that PTZ activates the PI3K/Akt/mTOR signaling cascades and FUS pulsation affects the PTZ-induced activation of Akt/mTOR/S6 (a potential molecular pathway is summarized in Fig. S4). More evidence is needed to support the understanding of the entire biophysical–biochemical mechanism in ultrasound-related epileptic discharge suppression, and more studies are needed to comprehensively elaborate the true mechanism of ultrasound neuromodulation in epilepsy treatment.

PTZ injected rats display brief myoclonic jerks or freezing, but this is resolved within 5 min following the epileptic episode [26]. The concentration of PTZ in plasma from dogs after intravenous injection displayed a biexponential decline and the average plasma half-life of PTZ is 1.4 h [49]. The number of epileptic bursts decreased in a time dependent manner (Figs. 3 and 4), similar to the time-dependent decline of epileptic EEG signal bursts in PTZ-induced rats found by Min [25]. These reports and results indicate a fast absorbance and elimination rate of PTZ in animals, and a single injection of PTZ induces acute epilepsy rather than chronic epilepsy.

Conclusion

This parametric study investigated valid ultrasound parameters for optimizing the suppression of epileptic neuronal activity, and confirmed that ultrasound pulsation effectively regulates the down-regulated PTZ-induced S6 phosphorylation as well as pAKT expression, thus confirming that ultrasound pulsation can temporally regulate the PI3K-Akt-mTOR pathway. Our findings provide solid evidence that focused ultrasound pulsation can serve as an effective noninvasive therapeutic tool to suppress epileptic activity and has high potential for clinical applications. The results provide an important reference for the development of focused ultrasound-based applications for epilepsy treatment or ultrasound neuromodulation potential for CNS disease intervention.

Funding sources

This study was supported by the Ministry of Science and Technology, Taiwan, under grants 105-2221-E–182-022,106-2221-E–182-02, 106-2410-H-182-008-MY2 and 108-2314-B-182-011 and by Chang Gung Memorial Hospital, Taiwan, under grants CIRPD2E0053 and CMRPD2D0113.

Declaration of competing interest

Hao-Li Liu provides technical consulting service for NaviFUS Inc. Taiwan, and he currently holds patents relates to biomedical ultrasound. The other authors declare no other conflicts of interests.

Appendix A. Supplementary data

Supplementary data to this article can be found online at https://doi.org/10.1016/j.brs.2019.09.011.

References

[1] Ding K, Gupta PK, Diaz-Arrastia R. Epilepsy after traumatic brain injury. In: Laskowitz D, Grant G, editors. Translational research in traumatic brain injury, Boca raton (FL); 2016.
[2] Kwan P, Brodie MJ. Refractory epilepsy: mechanisms and solutions. Expert Rev Neurother 2006;6(3):397–406.
[3] Vidyaratne LS, Iftekharuddin KM. Real-time epileptic seizure detection using EEG. IEEE Trans Neural Syst Rehabil Eng 2017;25(11):2146–56.
[4] Fisher RS, van Emde Boas W, Blume W, Elger C, Genton P, Lee P, et al. Epileptic seizures and epilepsy: definitions proposed by the international league against epilepsy (ILAE) and the international bureau for epilepsy (IBE). Epilepsia 2005;46(4):470–2.
[5] Abramovici S, Bagic A. Epidemiology of epilepsy. Handb Clin Neurol 2016;138:159–71.
[6] Fiest KM, Sauro KM, Wiebe S, Patten SB, Kwon CS, Dykeman J, et al. Prevalence and incidence of epilepsy: a systematic review and meta-analysis of international studies. Neurology 2017;88(3):296–303.
[7] Wong M. A critical review of mTOR inhibitors and epilepsy: from basic science to clinical trials. Expert Rev Neurother 2013;13(6):657–69.
[8] Ibrahim GM, Rutka JT, Snead 3rd OC. Epilepsy surgery in childhood: no longer the treatment of last resort. CMAJ (Can Med Assoc J) 2014;186(13):973–4.
[9] Engel Jr J. What can we do for people with drug-resistant epilepsy? The 2016 Wartenberg Lecture. Neurology 2016;87(23):2483–9.
[10] Rolston JD, Deng H, Wang DD, Englot DJ, Chang EF. Multiple subpial transections for medically refractory epilepsy: a disaggregated review of patient-level data. Neurosurgery 2018;82(5):613–20.
[11] Vicario CM, Nitsche MA. Non-invasive brain stimulation for the treatment of brain diseases in childhood and adolescence: state of the art, current limits and future challenges. Front Syst Neurosci 2013;7:94.
[12] Nitsche MA, Paulus W. Noninvasive brain stimulation protocols in the treatment of epilepsy: current state and perspectives. Neurotherapeutics 2009;6(2):244–50.
[13] Santiago-Rodriguez E, Cardenas-Morales L, Harmony T, Fernandez-Bouzas A, Porras-Kattz E, Hernandez A. Repetitive transcranial magnetic stimulation decreases the number of seizures in patients with focal neocortical epilepsy. Seizure 2008;17(8):677–83.
[14] Chen R, Spencer DC, Weston J, Nolan SJ. Transcranial magnetic stimulation for the treatment of epilepsy. Cochrane Database Syst Rev 2016;8:CD011025.
[15] Reithler J, Peters JC, Sack AT. Multimodal transcranial magnetic stimulation: using concurrent neuroimaging to reveal the neural network dynamics of noninvasive brain stimulation. Prog Neurobiol 2011;94(2):149–65.
[16] Nitsche MA, Cohen LG, Wassermann EM, Priori A, Lang N, Antal A, et al. Transcranial direct current stimulation: state of the art 2008. Brain Stimul 2008;1(3):206–23.
[17] Woods AJ, Antal A, Bikson M, Boggio PS, Brunoni AR, Celnik P, et al. A technical guide to tDCS, and related non-invasive brain stimulation tools. Clin Neurophysiol 2016;127(2):1031–48.
[18] Bowary P, Greenberg BD. Noninvasive focused ultrasound for neuromodulation: a review. Psychiatr Clin N Am 2018;41(3):505–14.
[19] Rezayat E, Toostani IG. A review on brain stimulation using low intensity focused ultrasound. Basic Clin Neurosci 2016;7(3):187–94.
[20] Dallapiazza RF, Timbie KF, Holmberg S, Gatesman J, Lopes MB, Price RJ, et al. Noninvasive neuromodulation and thalamic mapping with low-intensity focused ultrasound. J Neurosurg 2018;128(3):875–84.
[21] Lee W, Lee SD, Park MY, Foley L, Purcell-Estabrook E, Kim H, et al. Image-guided focused ultrasound-mediated regional brain stimulation in sheep. Ultrasound Med Biol 2016;42(2):459–70.
[22] Tyler WJ, Tufail Y, Finsterwald M, Tauchmann ML, Olson EJ, Majestic C. Remote excitation of neuronal circuits using low-intensity, low-frequency ultrasound. PLoS One 2008;3(10):e3511.
[23] Tyler WJ, Lani SW, Hwang GM. Ultrasonic modulation of neural circuit activity. Curr Opin Neurobiol 2018;50:222–31.

[24] Legon W, Bansal P, Tyshynsky R, Ai L, Mueller JK. Transcranial focused ultrasound neuromodulation of the human primary motor cortex. Sci Rep 2018;8(1):10007.
[25] Min BK, Bystritsky A, Jung KI, Fischer K, Zhang Y, Maeng LS, et al. Focused ultrasound-mediated suppression of chemically-induced acute epileptic EEG activity. BMC Neurosci 2011;12:23.
[26] Zhang B, Wong M. Pentylenetetrazole-induced seizures cause acute, but not chronic, mTOR pathway activation in rat. Epilepsia 2012;53(3):506–11.
[27] Sha LZ, Xing XL, Zhang D, Yao Y, Dou WC, Jin LR, et al. Mapping the spatio-temporal pattern of the mammalian target of rapamycin (mTOR) activation in temporal lobe epilepsy. PLoS One 2012;7(6):e39152.
[28] Liu J, Reeves C, Michalak Z, Coppola A, Diehl B, Sisodiya SM, et al. Evidence for mTOR pathway activation in a spectrum of epilepsy-associated pathologies. Acta Neuropathol Commun 2014;2:71.
[29] Purtell H, Dhamne SC, Gurnani S, Bainbridge E, Modi ME, Lammers SHT, et al. Electrographic spikes are common in wildtype mice. Epilepsy Behav 2018;89:94–8.
[30] Dhamne SC, Ekstein D, Zhuo Z, Gersner R, Zurakowski D, Loddenkemper T, et al. Acute seizure suppression by transcranial direct current stimulation in rats. Ann Clin Transl Neurol 2015;2(8):843–56.
[31] Paxinos G, Watson C. The rat brain in stereotaxic coordinates. fifth ed. Amsterdam: Elsevier Academic Press; 2005.
[32] Tang CH, Lu DY, Tan TW, Fu WM, Yang RS. Ultrasound induces hypoxia-inducible factor-1 activation and inducible nitric-oxide synthase expression through the integrin/integrin-linked kinase/Akt/mammalian target of rapamycin pathway in osteoblasts. J Biol Chem 2007;282(35):25406–15.
[33] Wang Y, Liu X, Wang Y, Chen J, Han T, Su L, et al. Attenuation of pentylenetrazole-induced acute status epilepticus in rats by adenosine involves inhibition of the mammalian target of rapamycin pathway. Neuroreport 2017;28(15):1016–21.
[34] King RL, Brown JR, Newsome WT, Pauly KB. Effective parameters for ultrasound-induced in vivo neurostimulation. Ultrasound Med Biol 2013;39(2):312–31.
[35] Ye PP, Brown JR, Pauly KB. Frequency dependence of ultrasound neurostimulation in the mouse brain. Ultrasound Med Biol 2016;42(7):1512–30.
[36] Manlapaz JS, Åström KE, Ballantine HT, Lele PP. Effects of ultrasonic radiation in experimental focal epilepsy in the cat. Exp Neurol 1964;10(4):345–56.
[37] Hakimova H, Kim S, Chu K, Lee SK, Jeong B, Jeon D. Ultrasound stimulation inhibits recurrent seizures and improves behavioral outcome in an experimental model of mesial temporal lobe epilepsy. Epilepsy Behav 2015;49:26–32.
[38] Fomenko A, Neudorfer C, Dallapiazza RF, Kalia SK, Lozano AM. Low-intensity ultrasound neuromodulation: an overview of mechanisms and emerging human applications. Brain Stimul 2018;11(6):1209–17.
[39] Trippe J, Mix A, Aydin-Abidin S, Funke K, Benali A. Theta burst and conventional low-frequency rTMS differentially affect GABAergic neurotransmission in the rat cortex. Exp Brain Res 2009;199(3–4):411–21.
[40] Walls AB, Nilsen LH, Eyjolfsson EM, Vestergaard HT, Hansen SL, Schousboe A, et al. GAD65 is essential for synthesis of GABA destined for tonic inhibition regulating epileptiform activity. J Neurochem 2010;115(6):1398–408.
[41] Huang RQ, Bell-Horner CL, Dibas MI, Covey DF, Drewe JA, Dillon GH. Pentylenetetrazole-induced inhibition of recombinant gamma-aminobutyric acid type A (GABA(A)) receptors: mechanism and site of action. J Pharmacol Exp Ther 2001;298(3):986–95.
[42] Bialer M, White HS. Key factors in the discovery and development of new antiepileptic drugs. Nat Rev Drug Discov 2010;9(1):68–82.
[43] Ostendorf AP, Wong M. mTOR inhibition in epilepsy: rationale and clinical perspectives. CNS Drugs 2015;29(2):91–9.
[44] Jalali S, Huang Y, Dumont DJ, Hynynen K. Focused ultrasound-mediated bbb disruption is associated with an increase in activation of AKT: experimental study in rats. BMC Neurol 2010;10:114.
[45] Pankov R, Cukierman E, Clark K, Matsumoto K, Hahn C, Poulin B, et al. Specific beta1 integrin site selectively regulates Akt/protein kinase B signaling via local activation of protein phosphatase 2A. J Biol Chem 2003;278(20):18671–81.
[46] Ivaska J, Nissinen L, Immonen N, Eriksson JE, Kahari VM, Heino J. Integrin 2 1 promotes activation of protein phosphatase 2A and dephosphorylation of Akt and glycogen synthase Kinase 3. Mol Cell Biol 2002;22(5):1352–9.
[47] Raab-Graham KF, Haddick PC, Jan YN, Jan LY. Activity- and mTOR-dependent suppression of Kv1.1 channel mRNA translation in dendrites. Science 2006;314(5796):144–8.
[48] Niere F, Raab-Graham KF. mTORC1 is a local, postsynaptic voltage sensor regulated by positive and negative feedback pathways. Front Cell Neurosci 2017;11:152.
[49] Jun HW. Pharmacokinetic studies of pentylenetetrazol in dogs. J Pharm Sci 1976;65(7):1038–41.